AFOSR-TR-97

0586

REPORT DOCUMENTATION PAGE

1. AGENCY USE ONLY *(Leave blank)*	2. REPORT DATE	3. REPORT TYPE AND DATES COVERED
	24 Oct 97	Final Technical Report 3/1/95-6/30/97

4. TITLE AND SUBTITLE

Contributions of Shear Coaxial Injectors to Liquid Rocket Motor Combustion Instabilities

5. FUNDING NUMBERS

PE - 61102F
PR - 2308
SA - AS
G - F49620-95-1-0184

6. AUTHOR(S)

Michael M. Micci

7. PERFORMING ORGANIZATION NAME(S) AND ADDRESS(ES)

Department of Aerospace Engineering
The Pennsylvania State University
233 Hammond Bldg.
University Park, PA 16802

8. PERFORMING ORGANIZATION REPORT NUMBER

9. SPONSORING/MONITORING AGENCY NAME(S) AND ADDRESS(ES)

AFOSR/NA
110 Duncan Avenue, Suite B115
Bolling AFB, DC 20332-0001

10. SPONSORING/MONITORING AGENCY REPORT NUMBER

11. SUPPLEMENTARY NOTES

12a. DISTRIBUTION AVAILABILITY STATEMENT

Approved for public release; distribution is unlimited.

12b. DISTRIBUTION CODE

13. ABSTRACT *(Maximum 200 words)*

Acoustic oscillations were induced in a sub-scale liquid rocket engine that burned liquid oxygen and gaseous hydrogen as propellants. The oscillations in the chamber were forced by a rotating gear just downstream of the nozzle throat. High frequency data was acquired for pressure and velocity via a pressure transducer and a magnetic flowmeter. The magnetic flowmeter obtains the acoustic gas velocity by measuring the voltage induced by the ionized combustion products moving through an externally imposed magnetic field. A cross correlation was performed on the velocity and pressure signals to determine the amplitude and phase difference of the two signals. A linearized one-dimensional acoustic model was developed to simulate the mean and unsteady flow within the chamber with mass and energy addition. The phase difference between unsteady pressure and velocity was determined from the model and fit to match the phase difference measured by the experiments. The points where the modeled and experimental phase differences agreed determined the real part of the propellant evaporation and combustion pressure- and velocity-coupled response functions.

14. SUBJECT TERMS

liquid propellants, combustion stability

15. NUMBER OF PAGES

12

16. PRICE CODE

17. SECURITY CLASSIFICATION OF REPORT	18. SECURITY CLASSIFICATION OF THIS PAGE	19. SECURITY CLASSIFICATION OF ABSTRACT	20. LIMITATION OF ABSTRACT
Unclassified	Unclassified	Unclassified	UL

CONTRIBUTIONS OF SHEAR COAXIAL INJECTORS TO LIQUID ROCKET MOTOR COMBUSTION INSTABILITIES

Final Report
3/1/95 - 6/30/97

Grant No. F49620-95-1-0184

P.I.: Michael M. Micci
Department of Aerospace Engineering
The Pennsylvania State University
University Park, PA 16802

ABSTRACT

Acoustic oscillations were induced in a sub-scale liquid rocket engine that burned liquid oxygen and gaseous hydrogen as propellants. The oscillations in the chamber were forced by a rotating gear just downstream of the nozzle throat. High frequency data was acquired for pressure and velocity via a pressure transducer and a magnetic flowmeter. The magnetic flowmeter obtains the acoustic gas velocity by measuring the voltage induced by the ionized combustion products moving through an externally imposed magnetic field. A cross correlation was performed on the velocity and pressure signals to determine the amplitude and phase difference of the two signals. A linearized one-dimensional acoustic model was developed to simulate the mean and unsteady flow within the chamber with mass and energy addition. The phase difference between unsteady pressure and velocity was determined from the model and fit to match the phase difference measured by the experiments. The points where the modeled and experimental phase differences agreed determined the real part of the propellant evaporation and combustion pressure- and velocity-coupled response functions.

NOMENCLATURE

a	speed of sound (m/s)
B	magnetic flux density (T)
E	electric field strength (V/m)
f_k	frequency (Hz)
L	distance between electrodes in the magnetic flowmeter (m)
m_b	mass flux due to propellant mass and energy addition (kg/m^3s)
n_p	number of data points in average
p	pressure (Pa)
R_p	pressure-coupled response function
R_v	velocity-coupled response function
$\hat{S}(f)$	power spectra
T	temperature (K)
T_f	flame temperature (K)
V	voltage induced across electrodes in the magnetic flowmeter (V)
U,u	velocity of combustion gases (m/s)
x	distance along length of chamber (m)

Greek Symbols

α	proportionality constant for the magnetic flowmeter
ΔT	non-isentropic temperature change (K)
$\Delta\phi$	phase error (°)
γ	coherence

Superscripts

$\bar{}$ mean property

$\hat{}$ unsteady property as a function of x

Subscripts

p pressure

pu pressure and velocity correlation

u velocity

INTRODUCTION

Prior research has proven the validity of several techniques for analyzing combustion instabilities in liquid propellant rocket engines including the time lag concept and models of the actual combustion mechanisms[1]. Yet another technique defines response functions to determine combustion stability within the rocket chamber. When analyzing the stability of rocket engines, researchers determine the pressure- and velocity-coupled response functions. Each response function is a complex number which determines the response of the various processes within the rocket engine with respect to the unsteady pressure or velocity.

One method of determining the response functions is to measure the unsteady properties of the gases inside the rocket chamber. One technique used for solid propellants is the magnetic flowmeter. Micci and Caveny[2] determined the real part of the pressure-coupled response function in a forced longitudinal wave motor which burned solid propellants. A spinning gear at the exit of the rocket motor nozzle induced acoustic oscillations (unsteady pressure and velocity) within the motor. The experiments proved the validity of using a magnetic flowmeter in solid rockets independent of the propellant type. Wilson and Micci[3] implemented a similar experimental setup to measure the real and imaginary parts of the pressure-coupled response function. Response functions were found for two formulations of AP/HTPB composite propellants. Cauty, Comas, Vuillot and Micci[4] used a similar experimental setup to determine the real part of the pressure-coupled response function. This experiment deduced the response functions from the steady and unsteady pressure and the unsteady velocity. One experiment, completed by Holme[5], measured the steady velocity in the exhaust of a liquid rocket with an electromagnetic flowmeter. The flowmeter used the alternating magnetic field from an electromagnet. Holme concluded that the electromagnetic flowmeter worked properly for several types of liquid propellants excluding a hydrogen peroxide monopropellant due to its low flame temperature.

EXPERIMENTAL APPROACH

Sub-Scale Rocket Chamber

A sub-scale rocket chamber previously used to measure liquid oxygen drop size and velocity[6] was modified to include a segment which could measure unsteady pressure and velocity[7,8]. The design of the chamber was based on a single injection element of the Space Shuttle Main Engine (SSME) Preburner. Liquid oxygen was injected coaxially inside a surrounding gaseous hydrogen stream. The chamber was modular in design and consisted of six segments including, the injector, ignitor segment, pressure release mechanism, magnetic flowmeter segment, window segment and nozzle. The total length of the chamber was 0.377 m (14.8 in) and the width of the hexagonal cross-section from one face to the other was 0.028 m (1.12 in).

Acoustic oscillations were induced within the chamber by rotating a gear immediately downstream of the nozzle as shown in Figure 1. When the rotating teeth of the gear partially obstructed the flow from the converging nozzle the throat area was periodically varied. The gear was constructed of steel and contained 28 teeth. The height and width of the teeth, 0.0127 m (0.5 in), were approximately the same size as the diameter of the nozzle throat, 0.0132 m (0.52 in). A

protective steel box was constructed to contain and divert the exhaust gases away from the rocket chamber. The gear was driven by an explosion-proof motor which in turn was driven by an invertor. The invertor remotely controlled the frequency of the signal transmitted to the motor which controlled the motor speed.

Magnetic Flowmeter

Unsteady pressure and velocity measurements were acquired within the magnetic flowmeter segment of the rocket chamber. This segment contained a port for a high frequency pressure transducer to measure unsteady pressure and a magnetic flowmeter to measure unsteady velocity at 0.139 m (5.47 in) downstream of the injector. The magnetic flowmeter consisted of a permanent magnet and two electrodes. The interaction between the magnetic field and the electrically conducting combustion gas within the chamber induces a voltage across the electrodes.

From electromagnetic theory the electric field, E, is defined as $E = U \times B$ where U is the flow velocity of an electrically conducting fluid and B is the magnetic field. When two metal rods are placed in the electric field perpendicular to the direction of a gas flow a potential difference is generated. This potential difference is proportional to the product of the flow velocity and the magnetic field according to Faraday's Law[9]: $V = \alpha ULB$. In this equation α is a proportionality constant of the order 1, L is the distance between the electrodes and V is the induced voltage.

A cross sectional view of the magnetic flowmeter used in the experiments is shown in Figure 2. The path of the combusting gases passed through the magnetic flowmeter segment perpendicular to the page. The magnetic field was produced by a horseshoe permanent magnet with a gap density of 0.19 Tesla. The electrodes protruded into the chamber approximately 0.003 m (0.12 in) with the distance between them approximately 0.022 m (0.88 in).

Experimental Procedure

The hot fire combustion tests were conducted at the Cryogenic Combustion Laboratory at the Pennsylvania State University. For each test, high frequency pressure and velocity data were acquired from the piezoelectric pressure transducer and magnetic flowmeter. The gear which modulated the exhaust was rotated at a frequency between 2500 and 2700 teeth per second. These frequencies were near the first longitudinal resonance frequency of the chamber. The mean pressure for the tests ranged from 2.6 to 3.0 MPa (375 to 425 psi). Table 1 lists the actual operating conditions of each test.

Table 1 - Operating conditions of the experiments

Test No.	Pressure		Mixture Ratio	Velocity Ratio	Momentum Ratio	Liquid Reynolds No.	Weber No.	Frequency
	(psi)	(MPa)						(Hz)
Test 1	379	2.61	4.08	19.34	0.91	788,556	441,228	2,669
Test 2	400	2.76	3.82	20.16	1.01	774,704	463,969	2,540
Test 3	414	2.86	3.87	19.15	0.95	738,324	377,074	2,613
Test 4	429	2.96	4.94	14.24	0.55	830,486	271,594	2,607
Test 5	405	2.80	5.50	14.04	0.49	856,305	252,300	2,624
Test 6	410	2.83	5.29	14.50	0.53	899,763	316,532	2,568

EXPERIMENTAL RESULTS

The voltage difference measured by the magnetic flowmeter was converted into velocity as described in the previous section. The dimensionless proportionality constant, α, could not be determined and was assumed to be 0.5. For most of the tests the pressure signal oscillated between ±0.28 MPa (±40 psi) and the velocity signal had an average value between ±1.5 m/s (±5 ft/s). The pressure and velocity time records were transformed into the frequency domain by a

Fast Fourier Transform (FFT)[10] to calculate the Power Spectrum Density (PSD) of the pressure, $\hat{S}_p(f)$, and velocity, $\hat{S}_u(f)$, signals in the frequency domain. Figures 3 and 4 are plots of the PSD of the pressure and velocity signals for a test with a constant gear frequency of 2669 teeth per second. The data is plotted in three-dimensions on a waterfall plot to show dependence with time. Each horizontal line on the plot represents data taken over 0.178 seconds. The pressure PSD clearly shows the acoustic oscillations in the chamber at the frequency induced by the gear. Both the first and second harmonics are visible in the graph at approximately 2670 and 5340 Hz. As expected the velocity PSD is much noisier, however the induced frequency is still visible at both the first and second harmonics corresponding to the pressure wave.

The pressure and velocity signals were correlated to obtain the Cross Spectrum Density (CSD) between the pressure and velocity signals in the frequency domain. Figure 5 is a waterfall plot of the CSD for the same test shown in Figures 3 and 4. The CSD shows the pressure and velocity signals to be related at the gear forcing frequency and the plot is much less noisy than the waterfall plot of the velocity PSD. The CSD provided a means to calculate the phase difference between the pressure and velocity signals. The phase was calculated from the real and imaginary parts of the complex CSD frequency signal

The error associated with performing the CSD is determined by the coherence function as defined in Equation 1 where f_k is the frequency corresponding to the gear forcing frequency. The coherence is a ratio of the averaged CSD to the product of the measured pressure PSD and the measured velocity PSD. The coherence lies between the values of zero and one and equals one for a noiseless signal. Measured and averaged data have a coherence less than one. The coherence predicts the error in the CSD phase calculation. Equation 2 defines the phase error where n_p is the number of points over which the phase is averaged.

$$\gamma^2_{pu}(f_k) = \frac{\overline{\left|\hat{S}_{pu}(f_k)\right|}^2}{\hat{S}_p(f_k)\hat{S}_u(f_k)} \qquad (1)$$

$$\Delta\phi = \frac{\sqrt{1-\gamma^2_{pu}}}{\left|\gamma_{pu}\right|\sqrt{2n_p}} \qquad (2)$$

ACOUSTIC MODEL

Governing Equations

A linear one-dimensional acoustic model was derived to numerically solve for the mean and unsteady pressure and velocity within a distributed combustion rocket chamber following the work of Micci[11] for a solid rocket motor. The model starts with the governing equations for a one-dimensional, unsteady, compressible flow in a constant area rocket chamber. These equations include the continuity equation, conservation of momentum and energy, and the perfect gas law with mass and energy addition to describe the fluid properties of the products of combustion. The mass and energy addition is described by a mass flux term and is determined by the amount of liquid oxygen injected into the rocket chamber.

The governing equations are linearized by assuming each fluid property is the sum of a mean and a small perturbation value and is assumed to be sinusoidal in time. Terms of the order M^2 or less are neglected. The unsteady adiabatic flame temperature, $\hat{T}_f$, is described as the sum of an isentropic and non-isentropic unsteady temperature contribution as shown in Equation 3. The pressure- and velocity-coupled response functions for the liquid propellant evaporation and combustion are given in Equation 4.

$$\hat{T}_f(x) = \hat{T}(x) + \Delta\hat{T}(x) \tag{3}$$

$$R_p \frac{\hat{p}}{p} + R_v \frac{\hat{u}}{a} = \frac{\hat{m}_b}{m_b} + \frac{\Delta\hat{T}}{T_f} \tag{4}$$

Solution Technique

The five linearized equations given by the derivation of the model were solved simultaneously for different pressure- and velocity-coupled response functions given initial conditions. These initial conditions were set for the properties at the chamber wall near the injector. The initial condition for the mean density equaled the density of the hydrogen entering the chamber from the injector. The mean pressure was set to the mean chamber pressure. The unsteady velocity equaled zero at the injection wall of the chamber. The mean velocity was based on the injection velocity of the hydrogen into the chamber. The unsteady pressure was assumed to be approximately 10% of the mean chamber pressure. These initial conditions are summarized in Table 2.

In order to predict the conditions in the chamber the reaction was simulated with CHEMKIN[12] a well-stirred reactor model. The inputs included the chamber pressure, total propellant mass flow rate, chamber volume, fuel mass fraction, oxidizer mass fraction and equivalence ratio. The program predicted the adiabatic flame temperature and the mass fraction of the product species which allowed for the calculation of the gas properties, including the mixture molecular weight, the mixture gas constant, the ratio of specific heats and the speed of sound in the chamber.

The remaining parameters needed to solve the differential equations were the mass flux, frequency, and pressure- and velocity-coupled response functions. The mass flux source term in the governing equations was defined as the mass flow rate of LOX per chamber volume. The mass flux was assumed to be a parabolic function of downstream distance. The frequency was defined from the frequency corresponding to the maximum power on the CSD waterfall plots which was also the forcing frequency of the gear. The pressure- and velocity-coupled response functions were varied and will be discussed more in the next section.

RESULTS FROM MODEL

The model was solved for various real values of the pressure-coupled response function, R_p, and the velocity coupled response function, R_v. The results from the model predicted the phase difference between the unsteady pressure and velocity. The model was related to the experiment by comparing the phase difference of the model at 0.139 in (5.47 in) downstream of the injector face to the phase difference calculated from the CSD for the experiments. This distance of 0.14 m corresponds to the downstream position of the pressure transducer and magnetic flowmeter in the rocket chamber.

Table 2 - Initial conditions for linear acoustic model

Property	Initial Guess
$\bar{\rho}$	$\frac{P_{ch}}{RT_{ch}}$
$\bar{p}$	P_{ch}
$\hat{u}$	0
$\bar{u}$	$\frac{\dot{m}_{H_2}}{\rho_{H_2} A_{ch}}$
$\hat{p}$	$0.10P_{ch}$

A parametric study was completed by varying R_p and R_v for each test. Real integer values were used for each response function: R_p was varied between 0 and 5 and R_v ranged from 0 to 12. As the value of the response functions changes, the downstream location where the phase difference shifts from 90° to -90° also changes producing a range of values for the phase difference at 0.14 m. The phase difference shifts from a positive value at $R_v = 0$ to a negative value at $R_v = 12$. For values of R_p near zero the phase difference shifts from positive to negative through ±180° whereas for values of R_p near five the phase shifts through 0°. This particular phenomenon is observed because the model predicts the node of the pressure wave and hence the maximum unsteady velocity magnitude to be near the position of the magnetic flowmeter. By changing the values of the pressure- and velocity-coupled response functions the pressure node and velocity maximum may be moved slightly. This slight movement can strongly affect the phase difference between the unsteady pressure and velocity.

The experimental phase difference for each test was chosen based upon its coherence. Points corresponding to the highest coherence or the least amount of statistical error were compared to the phase difference computed by the model. By comparing the phase differences for each test to the model a range of values for R_p and R_v were found. For a phase difference of -60°, the model predicts a match where $R_p = 3, 4 \text{ or } 5$ and R_v is between 4 and 8.

The range for the pressure-coupled response function for each test is plotted in Figure 6. Test 1 in Figure 6 corresponds to the test discussed in the above text. The conditions of Tests 1, 2 and 3 are approximately the same as shown previously in Table 1. Likewise Test 4, 5 and 6 were run at similar conditions. The pressure-coupled response function for the conditions of Tests 4, 5 and 6 is between the range of zero and two. Although the range for R_p is quite large at any given frequency, for Tests 1, 2 and 3, R_p changes from between zero and two at 2540 Hz to between three and five at 2670 Hz.

A similar plot for the velocity-coupled response function is shown in Figure 7. This graph indicates that R_v decreases from between two and four at 2540 Hz to zero from 2610 to 2670 Hz for Tests 4, 5 and 6. The velocity-coupled response function ranges from four to eight for the frequency range between 2540 and 2670 Hz for Tests 1, 2 and 3.

CONCLUSIONS

A rotating gear near the exit of the nozzle of a sub-scale liquid rocket chamber induced acoustic oscillations within the chamber. Pressure transducers measured the mean and unsteady pressures within the chamber. A magnetic flowmeter equipped with a permanent magnet measured the unsteady velocity of the combusting gases. The experiments have proven that the magnetic flowmeter is capable of acquiring unsteady velocity data within a gaseous hydrogen/liquid oxygen rocket chamber.

The unsteady pressure and velocity time signals were transformed into the frequency domain with a Fast Fourier Transform. The two frequency signals were then correlated to determine the frequency at which both of the signals were oscillating, i.e. the forcing frequency of the rotating gear in the experiment. After averaging the phase difference between the unsteady pressure and velocity was determined at this frequency. The phase error was calculated from the coherence function at the forcing frequency.

A linearized one-dimensional acoustic model was developed to deduce the pressure- and velocity-coupled response functions corresponding to the experimental results. The equations derived from the model were solved for the mean density, pressure and velocity and the unsteady

pressure and velocity.. The flow properties measured during the experiment were input into the model as initial conditions.

The model predicted the phase difference between unsteady pressure and velocity for various real valued pressure- and velocity-coupled response functions. Response functions were found where the phase difference predicted by the model matched the phase difference calculated from the experiment. Each experimental phase difference chosen produced a range of values for the pressure- and velocity- coupled response functions. The real part of pressure-coupled response function ranged from zero to five and the real part of the velocity-coupled response function ranged from zero to twelve.

REFERENCES

1. Harrje, D. J. and Reardon, F. H. (ed.), Liquid Propellant Rocket Instability, NASA SP–194, 1972.

2. Micci, M. M. and Caveny, L. H.; "MHD Measurement of Acoustic Velocities in Rocket Motor Chambers," *AIAA Journal*, Vol. 20, No. 4, April 1982, pp. 516-521.

3. Wilson, J. R. and Micci, M. M.; "Direct Measurement of High Frequency, Solid Propellant, Pressure-Coupled Admittances," *Journal of Propulsion and Power*, Vol. 3, No. 4, July-August 1987, pp. 296-302.

4. Cauty, F., Comas, P., Vuillot F. and Micci, M. M.; "Magnetic Flow Meter Measurement of Solid Propellant Pressure-Coupled Responses Using an Acoustic Analysis," *Journal of Propulsion and Power*, Vol. 12, No. 2, 1995, pp. 436-438.

5. Holme, J. C., "Investigation of an Electromagnetic Technique for the Independent Measurement of Chemical Rocket Exhaust and Vector," Astrosystems International, Inc., Fairfield, NJ, AFFDL TR-65-98, June 1965.

6. Micci, M. M., Thomas, J.-L. and Glogowski, M.; "Shear Coaxial Injector Spray Combustion Experiments," 32nd JANNAF Combustion Meeting, Huntsville, Alabama, October 23-27, 1995.

7. Ferraro, M., Kujala, R. J., Thomas, J.-L., Glogowski, M. J. and Micci, M. M.; "Measurements of Shear Coaxial Injector Sprays: Cold Flow and Hot Fire Experiments," AIAA 96-3028, 32nd AIAA/ASME/SAE/ASEE Joint Propulsion Conference, Lake Buena Vista, Florida, July 1-3, 1996.

8. Micci, M. M., Kujala, R. J., Gandilhon, D., Ferraro, M. and Schmidt, M. G., "Unsteady Hot Fire Atomization Measurements in Injector Sprays," AIAA-97-2845, 33rd AIAA/ASME/SAE/ ASEE Joint Propulsion Conference, Seattle, WA, July 6-9, 1997.

9. Shercliff, J. A., Theory of Electromagnetic Flow-Measurement, Cambridge University Press, New York, 1962.

10. Bendat, J. S. and Piersol, A. G., Engineering Applications of Correlation and Spectral Analysis, 2nd Edition, John Wiley and Sons, Inc., New York, 1993.

11. Micci, M. M., "Linear Acoustic Analysis of Solid Propellant Pressure-Coupled Distributed Combustion," *Journal of Propulsion and Power*, Vol. 12, No. 6, 1996, pp. 1179-1181.

12. Sandia National Laboratories, CHEMKIN, 1996.

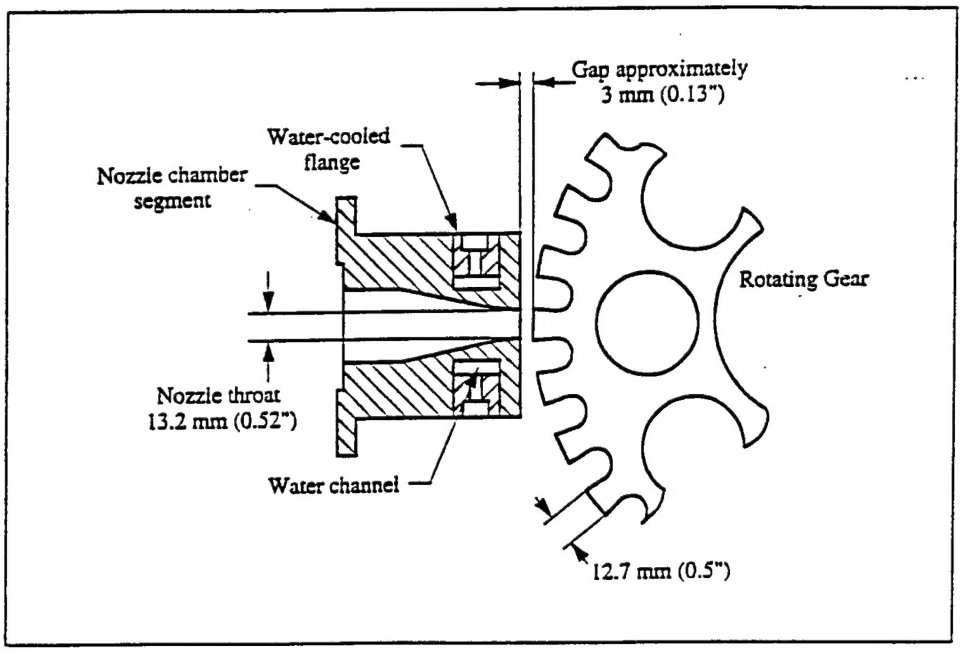

Figure 1 - Gear and nozzle setup

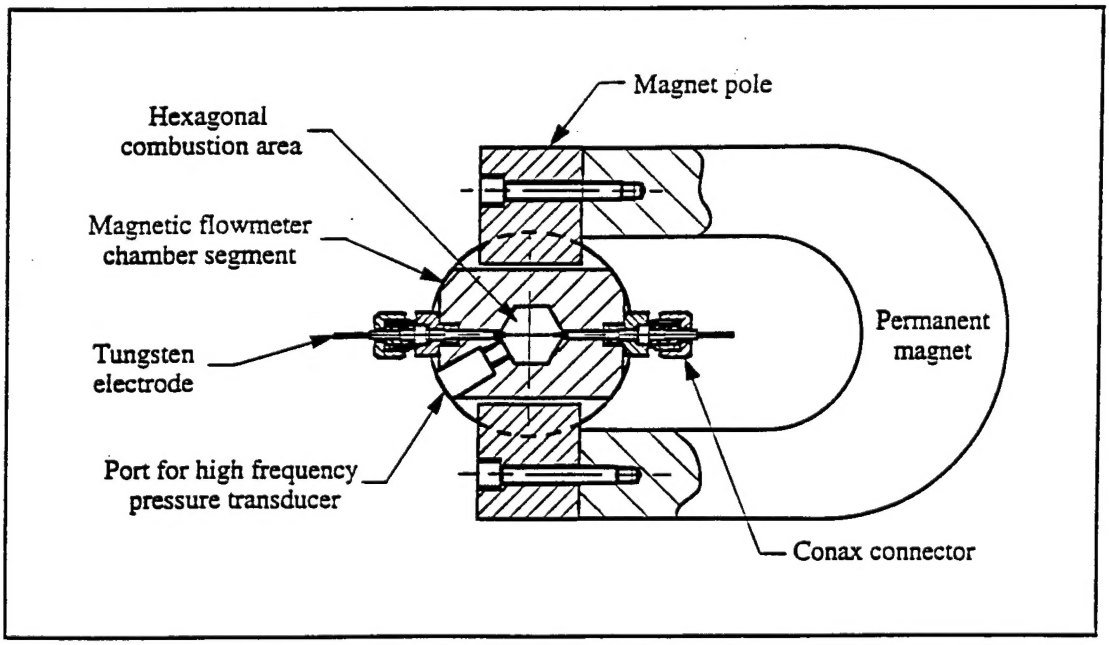

Figure 2 - Magnetic flowmeter chamber segment

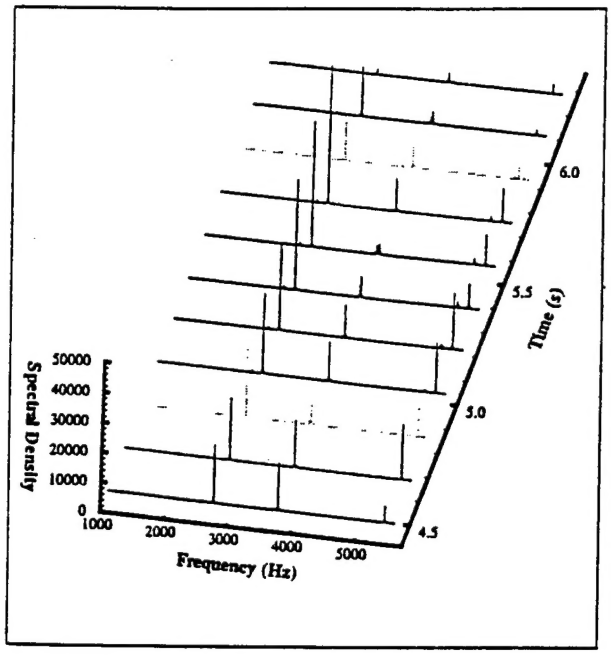

Figure 3 - Unsteady pressure power spectral density

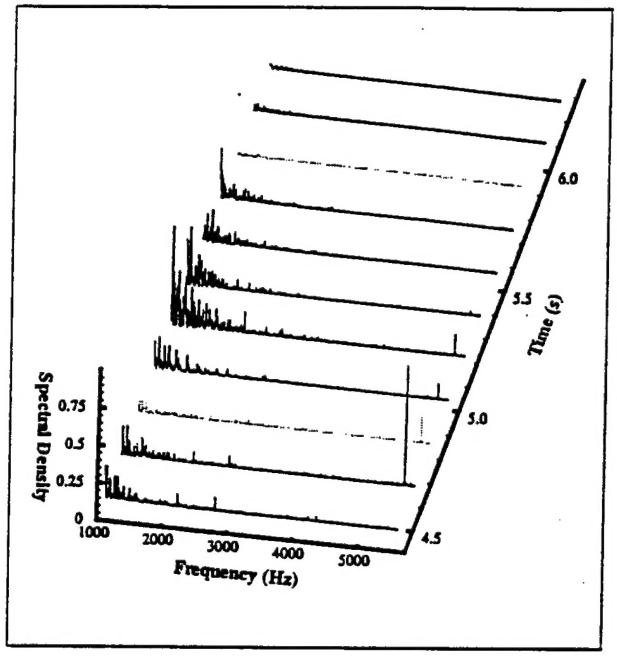

Figure 4 - Unsteady velocity power spectral density

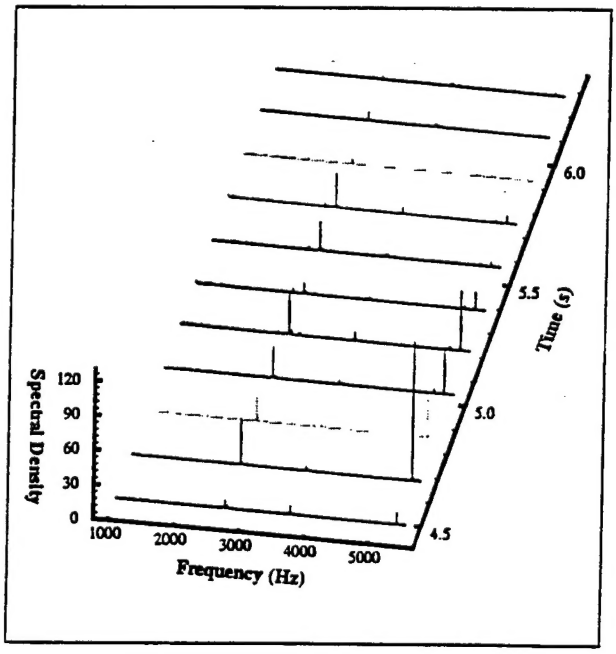

Figure 5 - Unsteady pressure and velocity cross spectral density

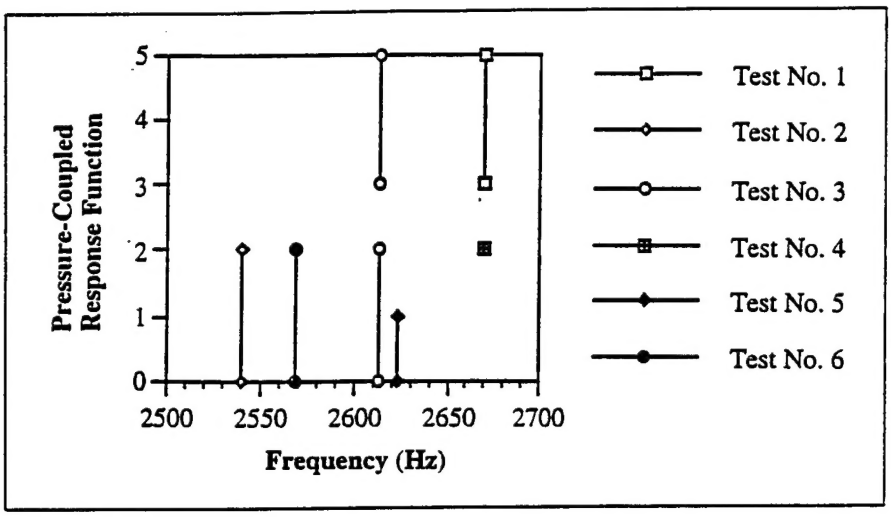

Figure 6 Pressure-coupled response function at different frequencies and test conditions.

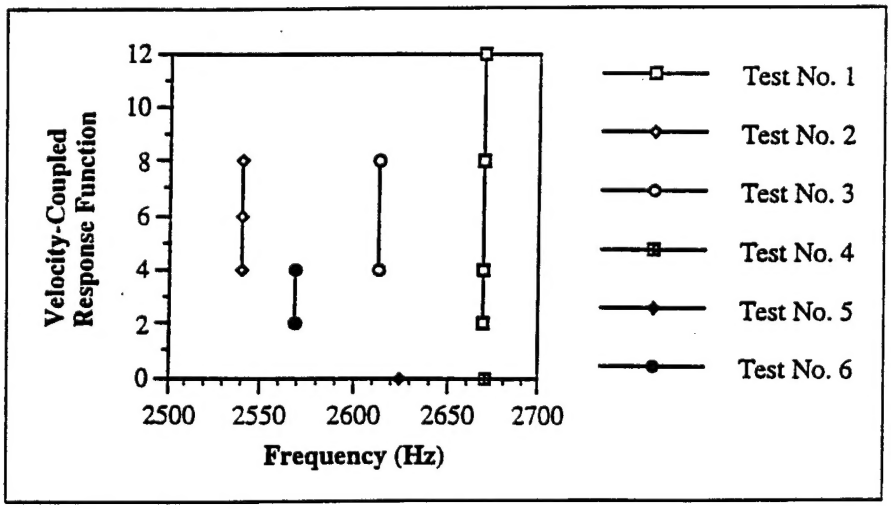

Figure 7 Velocity-coupled response function at different frequencies and test conditions.

PERSONNEL

Professional Staff

Michael M. Micci, Associate Professor, Aerospace Engineering

Graduate Students

Michael J. Glogowski, 1995-1996
Mena Ferraro, 1995-1997
Rodney Kujala, 1995-1997

PUBLICATIONS

"Experimental Characterization of Shear Coaxial Injectors Using Liquid/Gaseous Nitrogen," Puissant, C., Glogowski, M. J. and Micci, M. M., *Atomization and Sprays*, Vol. 7, No. 5, September-October 1997, pp. 467-478.

"Atomization of Coaxial-Jet Injectors," Ledoux, M., Micci, M., Glogowski, M., Vingert, L. and Gicquel, P. To be published in *Liquid Rocket Combustion Devices: Aspects of Modeling, Analysis and Design*, AIAA Progress in Astronautics and Aeronautics Series, Spring 1998.